Phase controlled one dimensional topological superconductivity

Ady Stern

Weizmann Institute of Science

With

1. Anna Keselman (Station Q), Erez Berg (Chicago, Weizmann)
   Falko Pientka, Bert Halperin, Amir Yacoby (Harvard) - PRX 2017

2. Arbel Haim (Cal-Tech) – PRL 2019

3. Erez Berg – PRL 2019

4. Setiawan Wenming and Erez Berg – Arxiv 2019

5. Collaboration with the QDEV experimentalists –
   A. Fornieri, F. Nichele, A. Drachmann, A. Whiticar, E. Porteles, C. Marcus, S. Wenming, A. Keselman (Nature, in Press)

Funding by: Microsoft’s Station Q, ERC, ISF, CRC183

Relevant papers by Hell et al., and Akhmerov et al.

Outline:

1. Introduction – Non-abelian states of matter
2. Background – 1D topological superconductivity
3. Going half a dimension higher – Planar Josephson junction
4. The (friendly!) effect of disorder
5. Fractionalization of Josephson vortices
6. Braiding Majorana zero modes in Josephson junctions

Non-abelian states of matter

A system with

1. A gapped spectrum
2. A degenerate ground state (protected degeneracy)

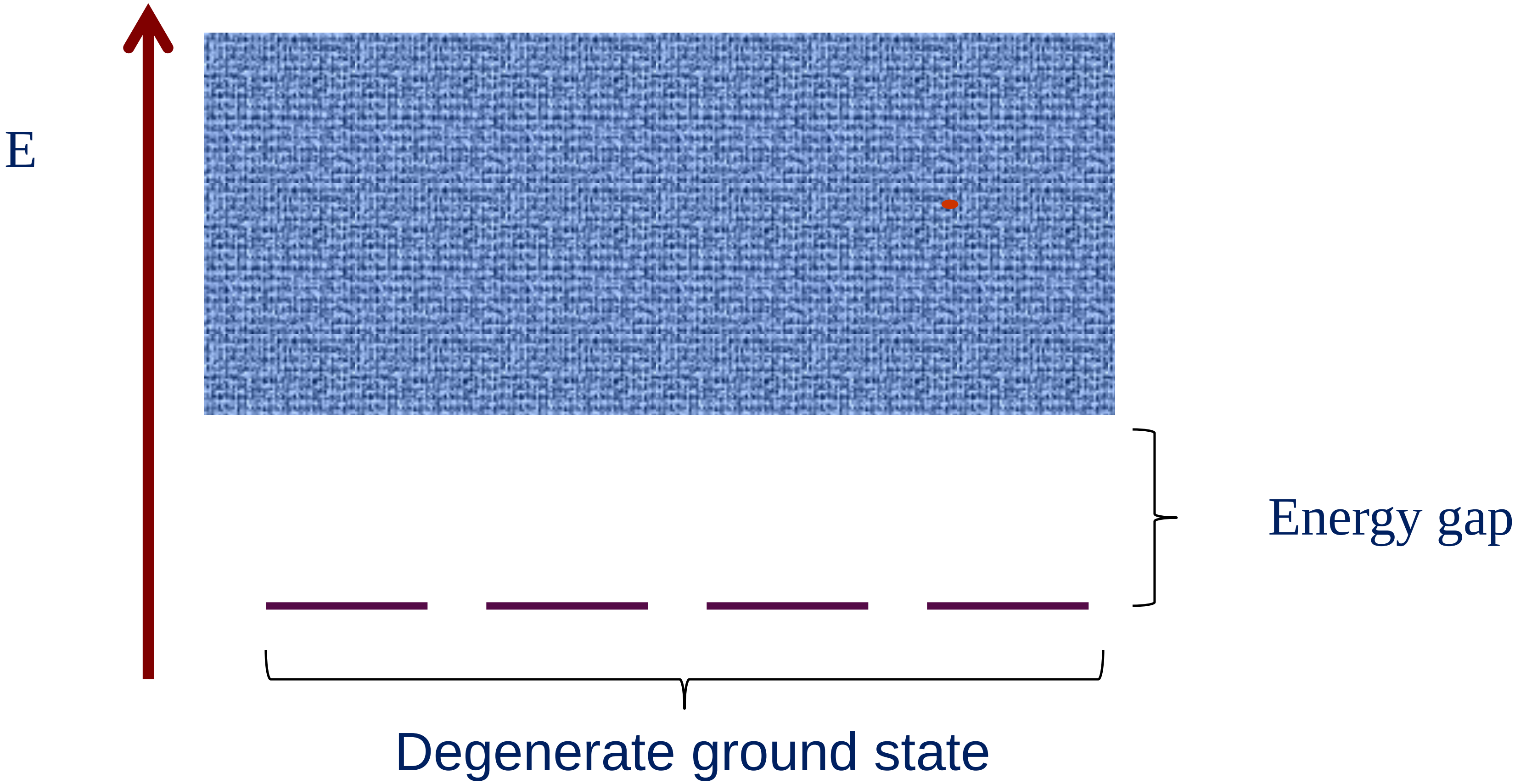

The degeneracy should be topologically protected -

The Hamiltonian:

$$\left(\begin{array}{c|c} 0 & 0 \quad \text{Non-zero} \\ \hline 0 \quad \text{Non-zero} & \text{Non-zero, but gapped} \end{array}\right)$$

Virtual transitions to excited states induce only exponentially small splitting between ground states, due to the energy gap

Introducing dynamics into the state by interchanging “quasi-particles”

Electrons

quasi-particles

A ground state: $\psi(r_1,\ldots\ldots\ldots\ldots r_k;\; R_1,..,R_N)$

Energy gap

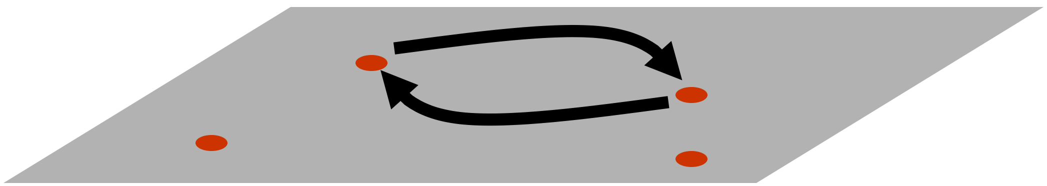

λ^N ground states

$|g.s.1(R_1,R_2,\ldots)\rangle$
$|g.s.2(R_1,R_2,\ldots)\rangle$
$\vdots$
$|g.s.\lambda^N(R_1,R_2,\ldots)\rangle$

R_1,R_2 ... position of quasi-particles

Interchange implements a unitary transformation within this subspace

Up to a global phase, the unitary transformation depends only on the topology of the trajectory

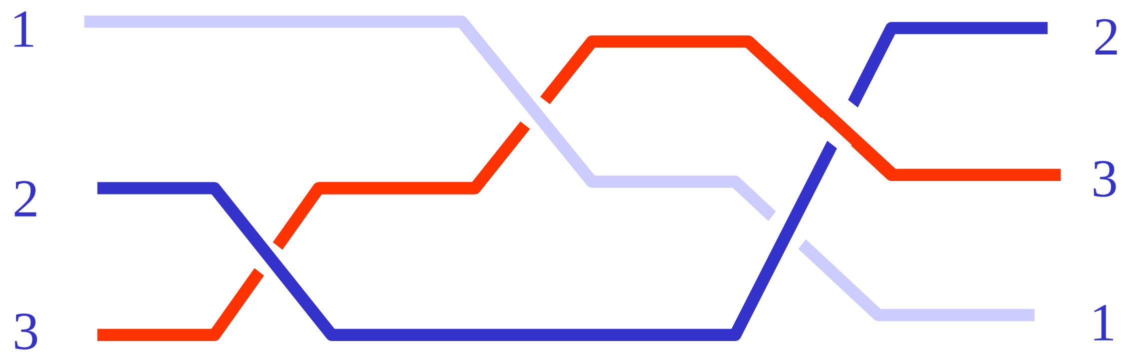

As robust as an electronic system gets…

Topological quantum computation (Kitaev 1997-2003)

- Subspace of degenerate ground states, separated by an energy gap from the continuum of excited states.
- Unitary transformations within this subspace are defined by the topology of braiding trajectories
  - immunity to errors
- Local operators do not couple between ground states
  – immunity to decoherence

Examples to non-abelian systems:

- Topologically protected localized zero energy excitations in superconductors, a.k.a. Majorana fermions
- Certain quantum Hall states (Moore-Read-Rezayi)

The simplest example – Majorana fermions in topological superconductors

(Kitaev, Read&Green, Kopnin, Saloma)

A superconductor at mean field theory is described by the BdG Hamiltonian

$$H = (\psi^+ \quad \psi)\begin{pmatrix} H_0 & \Delta \\ \Delta^+ & -H_0 \end{pmatrix}\begin{pmatrix} \psi \\ \psi^+ \end{pmatrix}$$

A quadratic Hamiltonian!

a matrix with two important properties:

- Even dimensional
- Spectrum is symmetric around zero energy

⇒ An even number of zero energy states

⇒ Two well separated zero energy modes are protected

- non-abelian static defects.
- May be realized in one dimensional wires and in vortex cores of two dimensional topological superconductors.

Properties –
The Majorana zero modes γ_i are unitary operators that satisfy

$$[H, \gamma_i] = 0$$
$$\gamma_i^2 = 1$$
$$\{\gamma_i, \gamma_j\} \propto \delta_{ij}$$
$$\gamma_i = \gamma_i^+$$

Span the subspace of degenerate ground states

Topological Superconductivity in Nanowires

Quantum wire with spin-orbit coupling and Zeeman field:

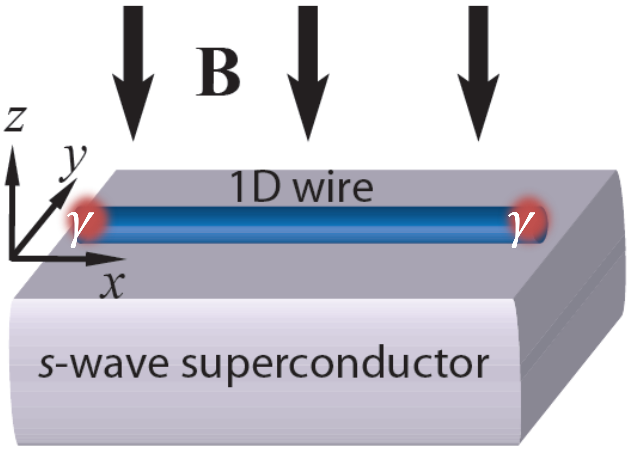

Lutchyn et al. PRL 2010
Oreg et al. PRL 2010

$$H_0 = \frac{k_x^2}{2m} - \mu + \alpha k_x \sigma_y + B\sigma_z$$

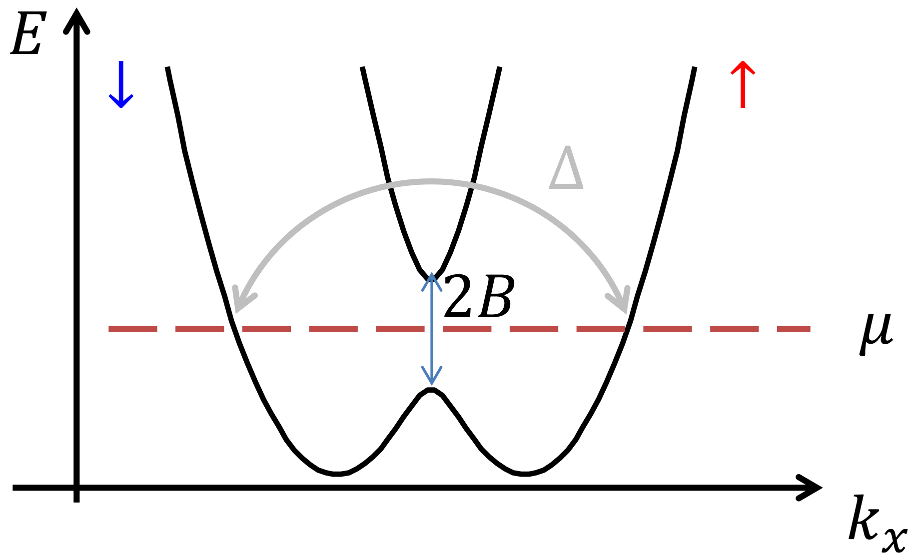

figure taken from
Alicea, Rep. Prog. Phys. (2012)

Requires fine-tuning of μ!

Topological Superconductivity in Nanowires

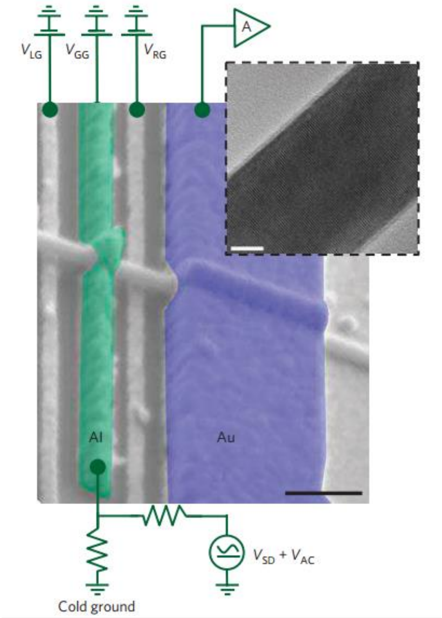

Das et al.,
Nature Physics 2012

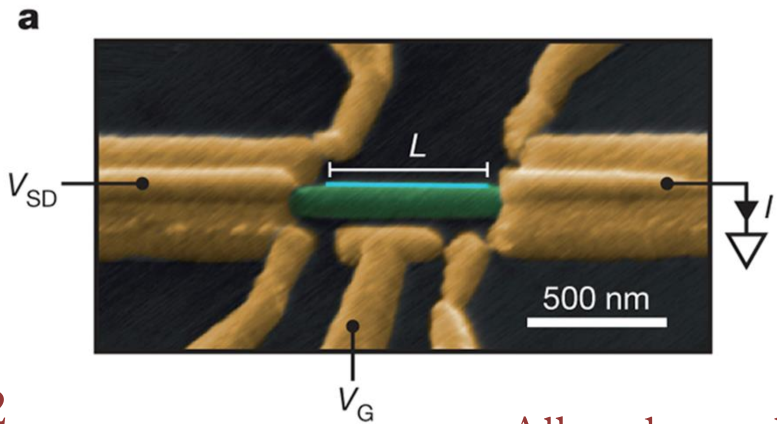

Albrecht et al.,
Nature 2016

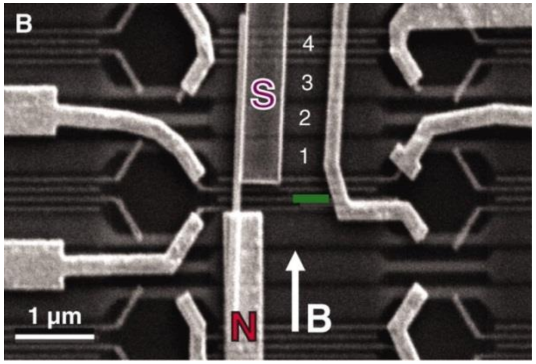

Mourik et al.,
Science 2012

Rokhinson et al., Nature Phys. (2012), Deng et al., Nano Lett. (2012), Churchill et al., Phys. Rev. B (2013), Nadj-Perge, Science (2014)

Topological superconductivity in planar Josephson junctions

Going half a dimension higher – 1D topological superconductor in a 2D setting

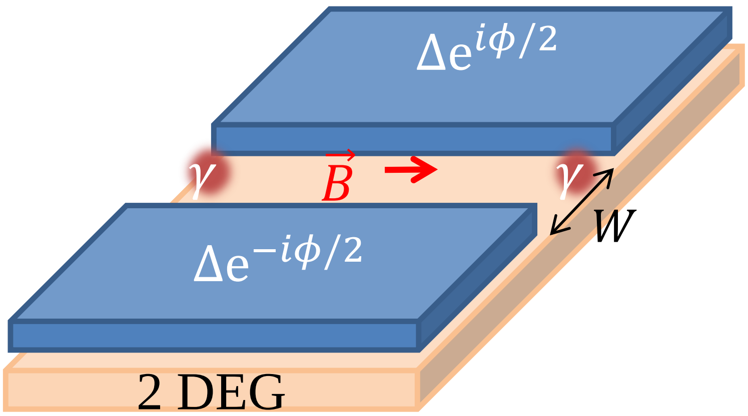

Ingredients:

✓ 1D
✓ Spin-orbit
✓ Superconductivity
✓ Magnetic field

New knobs to tune – phase difference, Josephson current, enclosed magnetic flux

New features:

- Robust topological phase with no fine-tuning (for $\phi \approx \pi$)
- Can tune itself the topological phase!

Robust topological phase with no fine-tuning (for $\phi \approx \pi$)

Phase difference

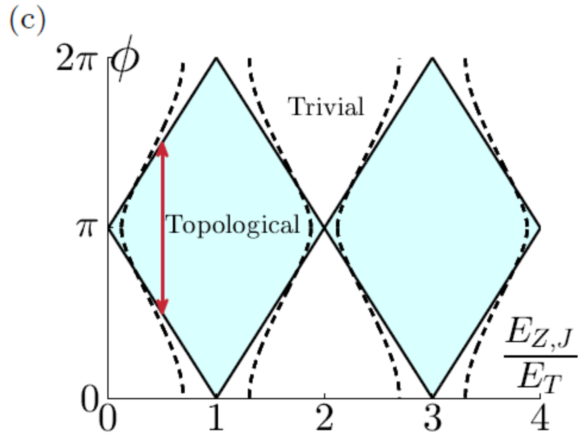

Zeeman energy * traversal time

Only weak dependence on the chemical potential
(Spin orbit energy >> Zeeman energy, wide superconductors)

First order phase transition between trivial and topological state – the system self tunes to the topological regime

The phase difference at the ground state:

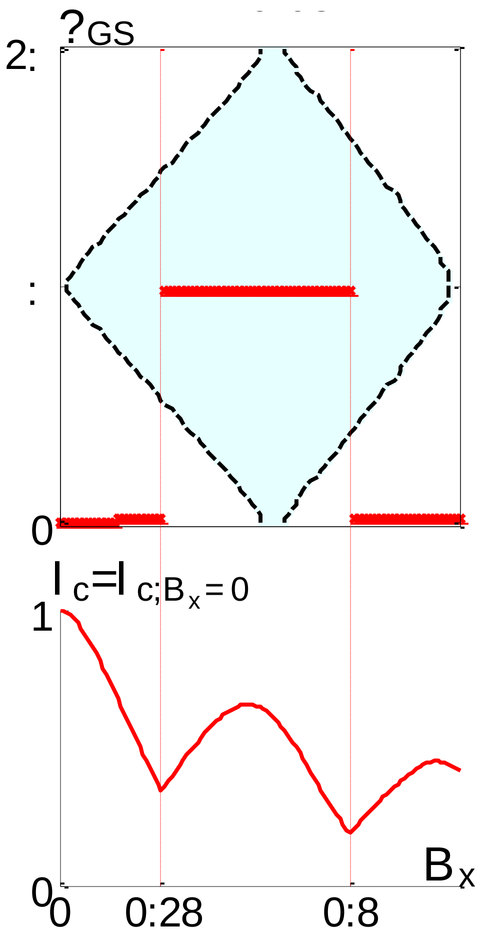

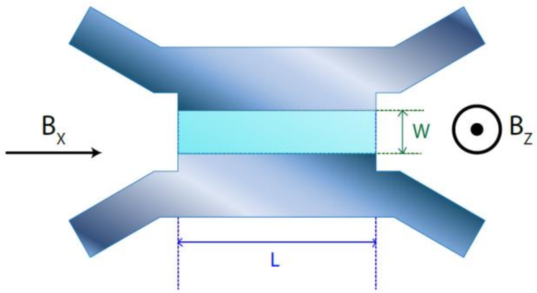

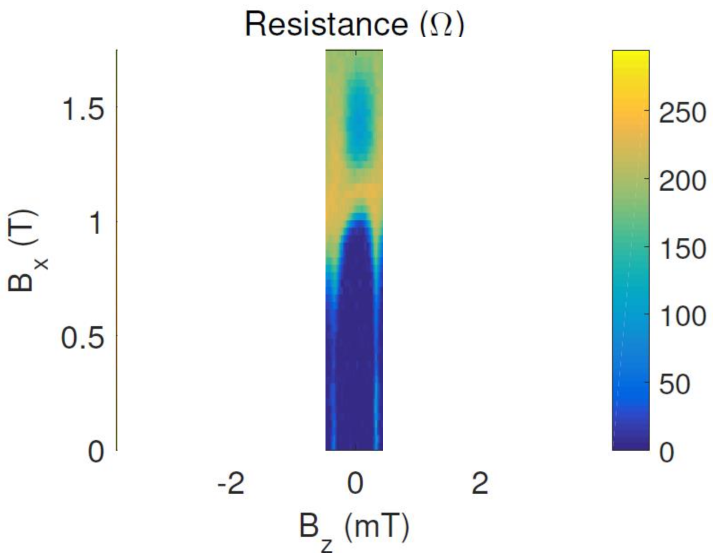

Hart et al. arXiv,1509.02940 (2015)

The transition coincides with a minimum of the critical current.

Setup and Model

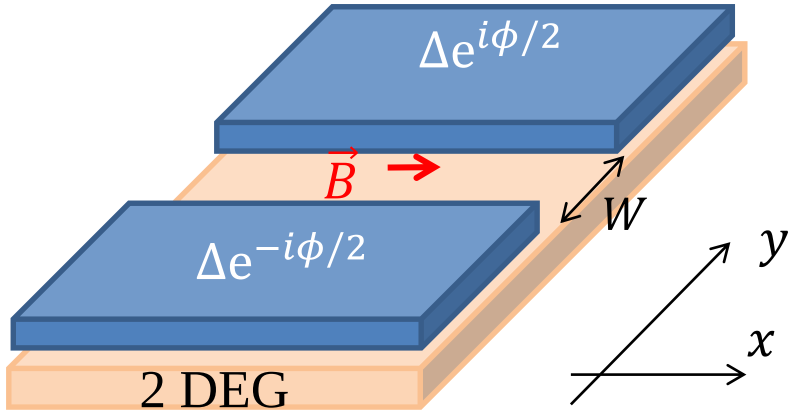

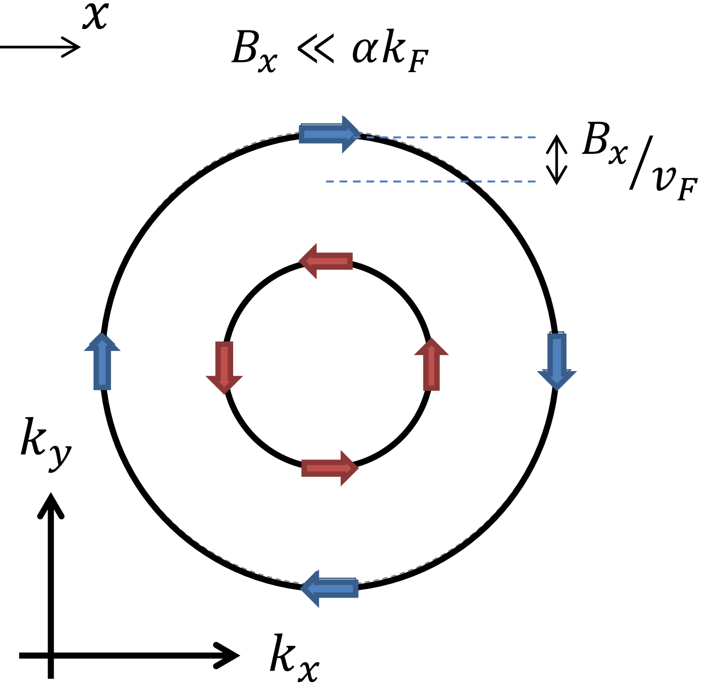

Hamiltonian in the normal region:

$$H_0 = \frac{k_x^2 + k_y^2}{2m} - \mu + \alpha\left(k_x\sigma_y - k_y\sigma_x\right) + B_x\sigma_x$$

$$H_0 = \frac{k_x^2 - \partial_y^2}{2m} - \mu + \alpha\left(k_x\sigma_y + i\partial_y\sigma_x\right) + B_x\sigma_x$$

We are looking for states within the gap, bound between the two superconductors

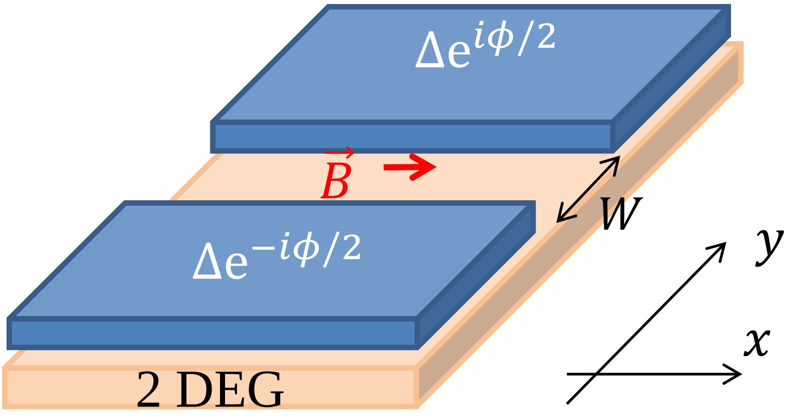

Almost the particle in the box problem, except the boundary conditions - Andreev processes

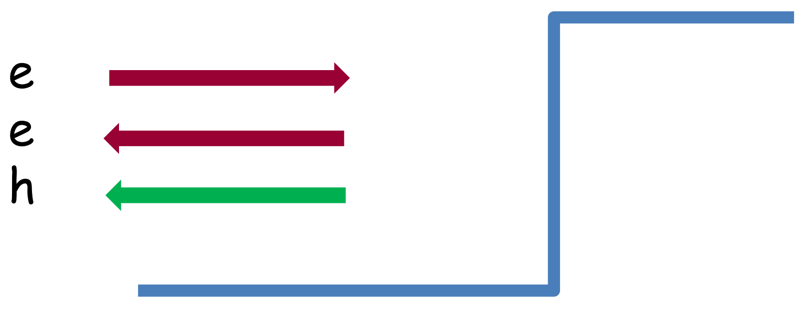

For distinguishing topological from trivial, we need to look at k_x=0

For the ground state energy and energy gap, we need all k_x

Topological invariant = fermion parity at k_x=0 Kitaev (2001)

$\Rightarrow$ Look for single gap closing at k_x=0

Andreev bound state spectrum, $\Delta \ll \mu$:

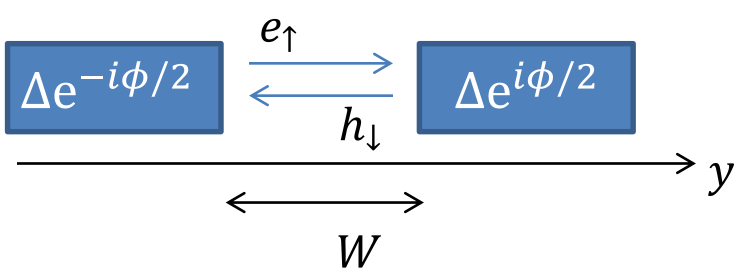

$$\underbrace{2\cos^{-1}\frac{E_n}{\Delta} + \phi}_{\text{phase acquired upon Andreev reflection}} + \underbrace{\cancel{2\frac{E_n}{v_F}W} \pm 2\frac{B_x}{v_F}W}_{\text{phase acquired upon traversing the junction}} = 2\pi n$$

Narrow junction, i.e. $\Delta \ll {}^{v_F}/_{W}$: $E_n = \Delta\cos\left(\frac{\phi}{2} \pm \frac{B_x}{v_F}W\right) = \Delta\cos(\frac{\phi}{2} \pm \phi_B)$

Phase Diagram

k_x=0 bound states:

$$E_n = \Delta\cos\left(\frac{\phi}{2} \pm \frac{B_x}{v_F}W\right)$$

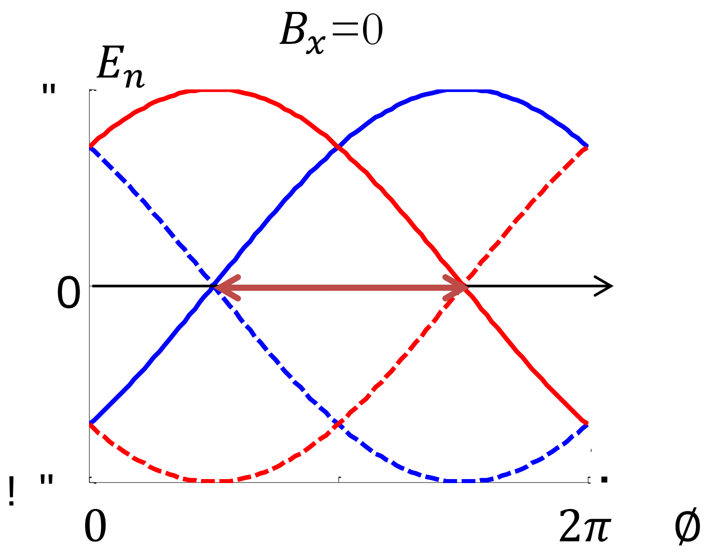

State is doubly degenerate!

Gap closing lines (for any W):

$$\phi \pm 2\frac{B_x}{v_F}W = (2n+1)\pi$$

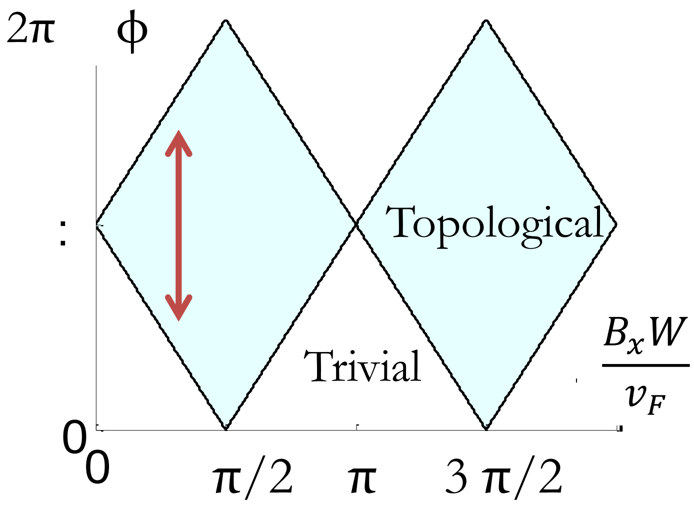

Insensitive to μ!

Majorana end states

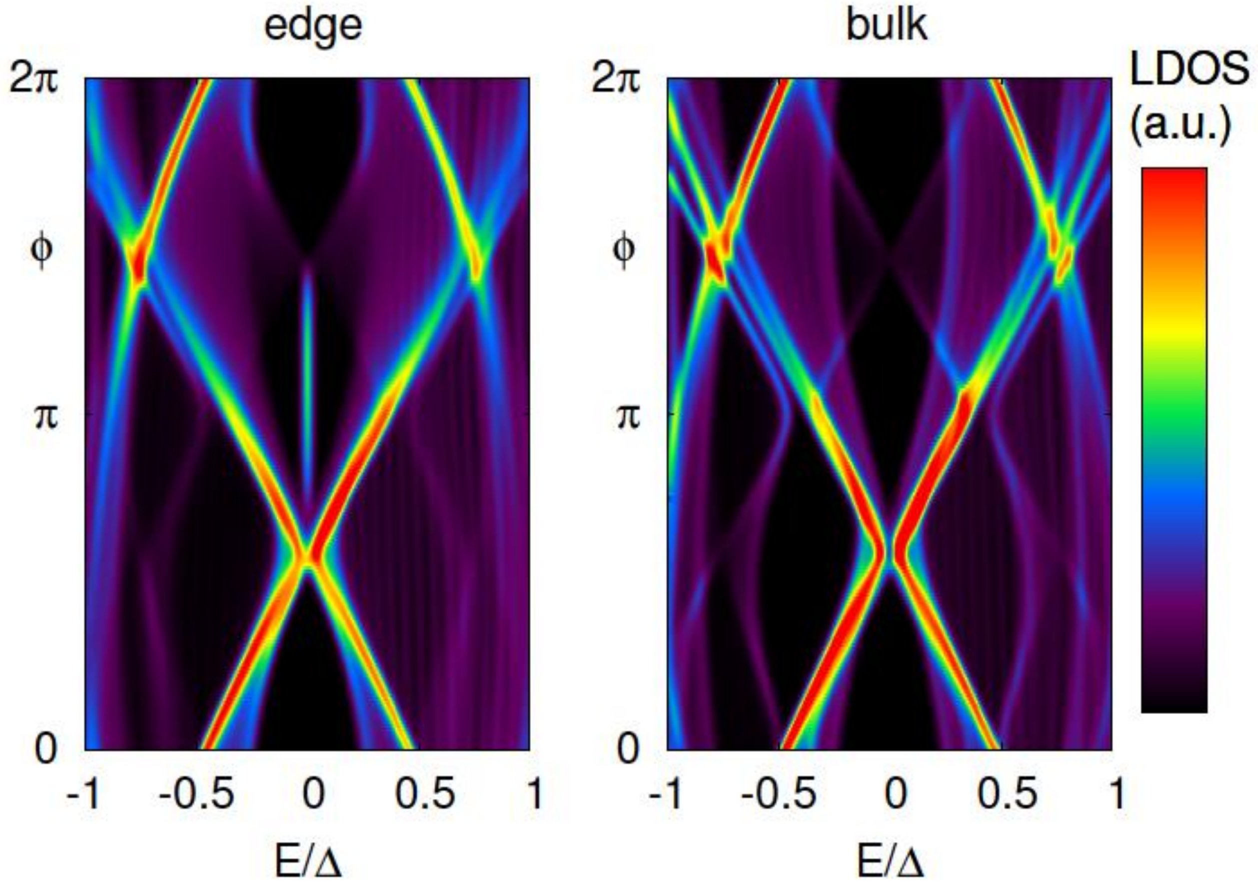

What if the superconductors are narrow?

(with Setiawan Wenming and Erez Berg, 2019)

Width of superconductor $\ll$ induced coherence length hv_F/Δ.

- Normal reflections from the interface with the vacuum ⇒ minimum field required for topological superconductivity.

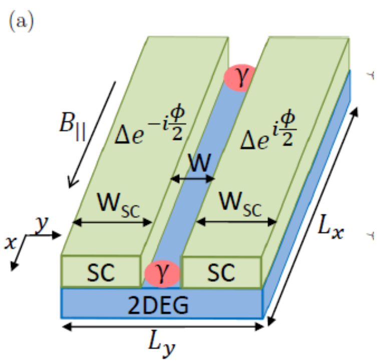

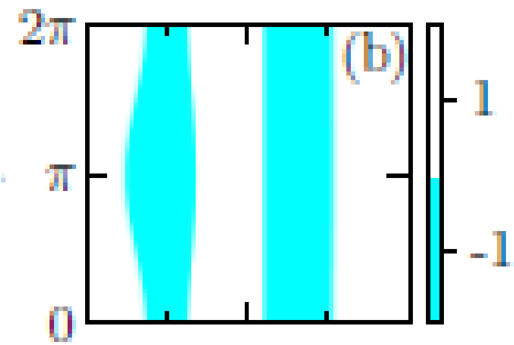

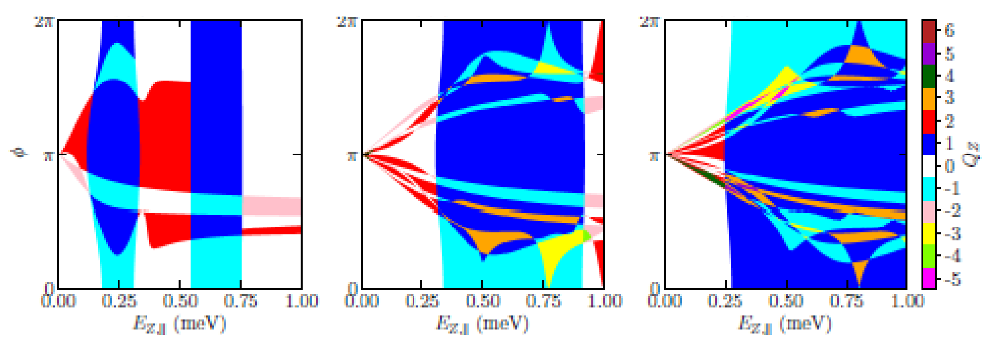

Experiments – Nichele - Marcus group (NBI)

Measuring the tunneling density of states
at the end of the junction

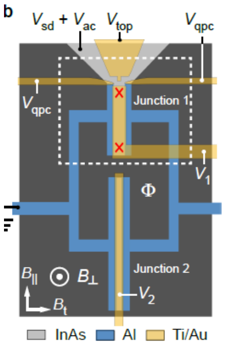

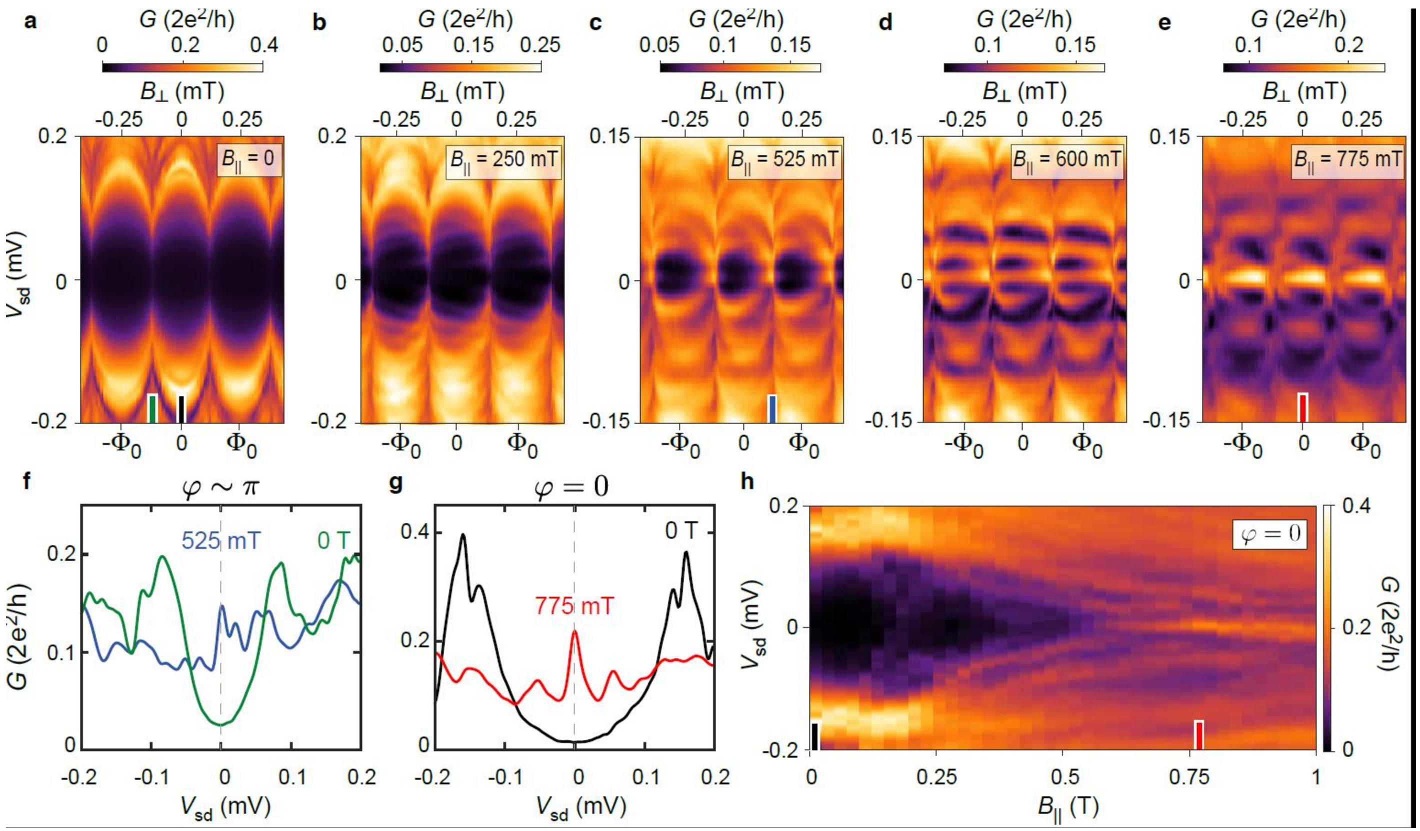

Experiments – Yacoby group (Harvard)

Measuring the tunneling density of states at the end of the junction

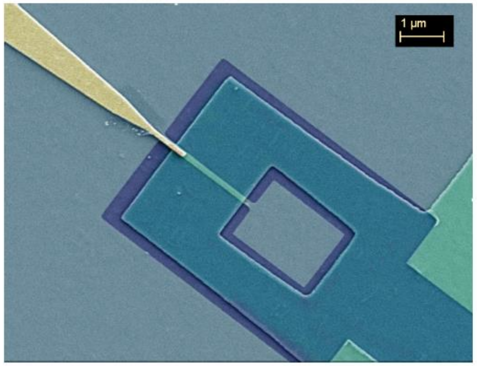

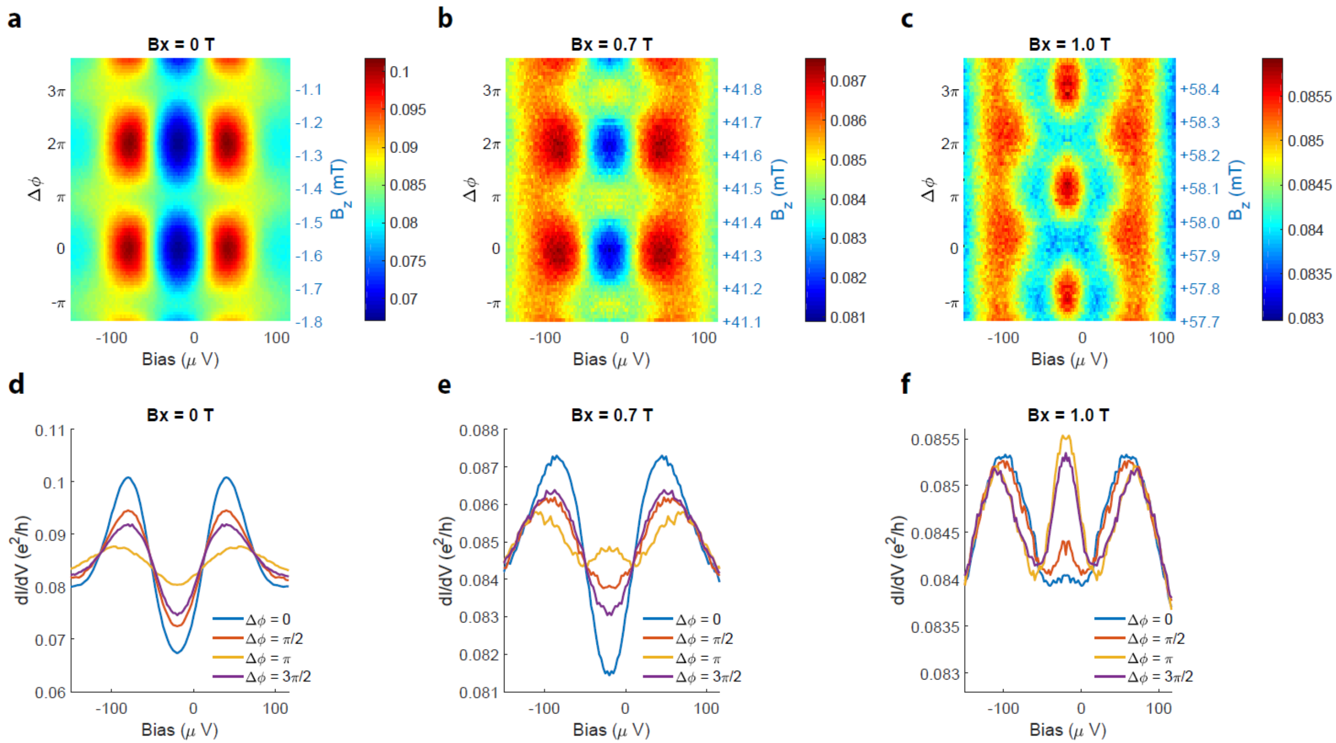

Experiments – Goswami group (Delft)

Measurement of the recovery of the critical current with increasing parallel magnetic field

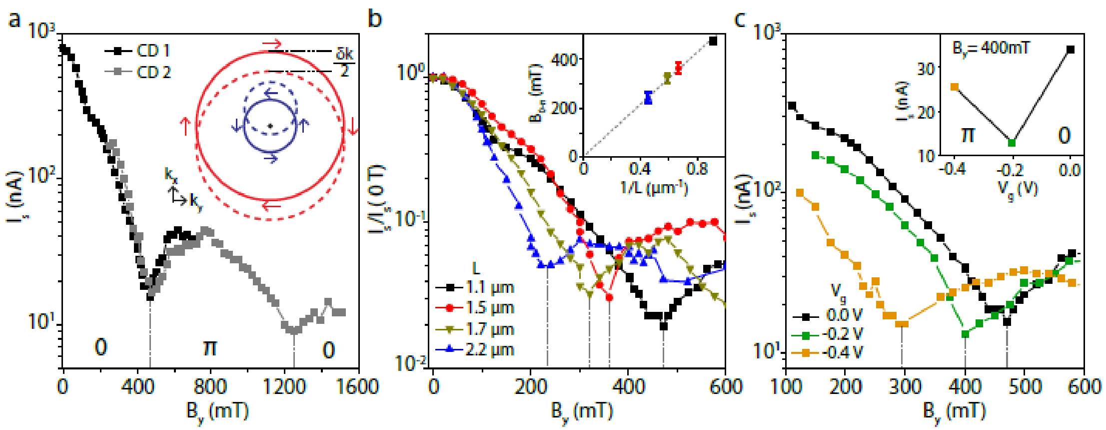

FIG. 2. | **Magnetic field-driven $0-\pi$ transitions. a,** Variation of the switching current, I_s, with in-plane magnetic field, B_y, at $V_g = 0$ V for the same JJ as in Fig. 1b,c. Two distinct revivals of I_s are visible at $B_y = 470$ mT and 1250 mT, associated with $0-\pi$ transitions. The data is from two cool downs (CDs). The momentum shift, $\delta k/2$, of the Fermi surfaces due to the Zeeman field is sketched in the inset. The solid (dashed) lines depict the situation at zero (finite) magnetic field, and the arrows represent the spin orientation. **b,** I_s as a function of B_y at $V_g = 0$ V for four JJs with different lengths. For better visibility, I_s is normalized with respect to I_s at $B_y = 0$ T. Dashed lines indicate $B_{0-\pi}$, the field at which the transition occcurs for each length. The inset shows a linear dependence of $B_{0-\pi}$ on $1/L$, in agreement with ballistic transport. **c,** I_s vs. B_y at three different V_g for the JJ with $L = 1.1$ μm. $B_{0-\pi}$ shifts to lower values of B_y with more negative gate voltages. I_s vs. V_g at $B_y = 400$ mT shows a non-monotonic behavior as displayed in the inset. The length and gate dependence of panel **b** and **c** are in qualitative agreement with Eq. 1.

The effect of disorder on the localization of the zero modes

With Arbel Haim (Cal-Tech)
Arxiv 1808.07886

Numerically -

For weak disorder, Majoranas get (significantly) better localized.

In contrast to 1D p-wave superconductors.

Why –

1. Identify the culprit – large k gap

2. The effect of disorder on that gap – combination of selection rules and pairing phases.

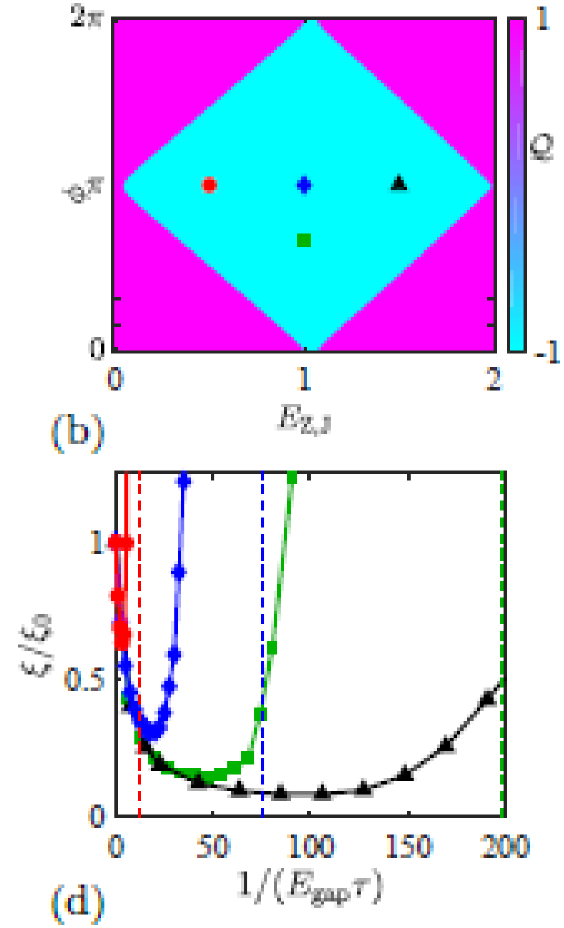

Spectrum of excitations in the topological phase

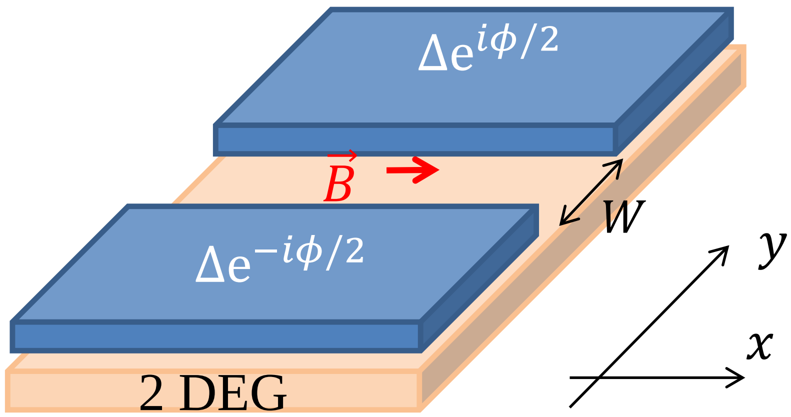

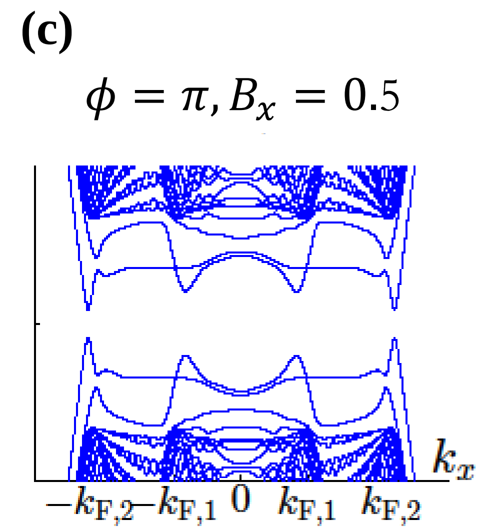

Smallest gap at the two Fermi momenta

Think about the spectrum as coming from pairing of several modes

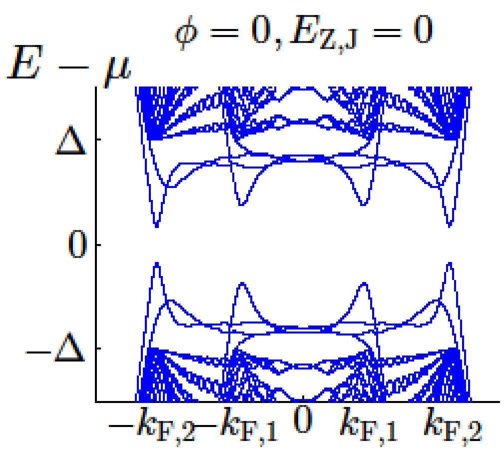

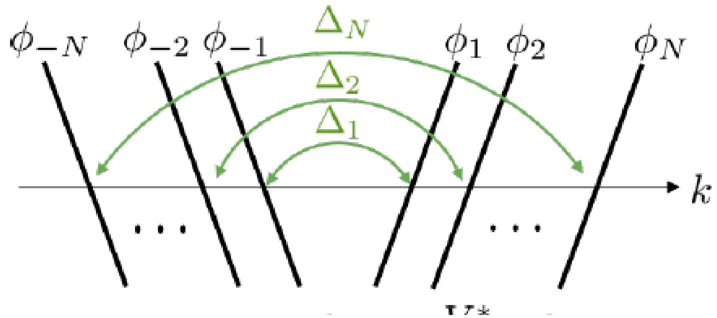

Effect of disorder - perturbative calculation:

Localization length - $\frac{hv_F}{\Delta_{eff}}$

$$\Delta_{eff,m} \approx \Delta_m + \sum_{n \neq m} \frac{1}{\tau_{mn}} e^{i \arg(\Delta_n) + i\alpha_{mn}} \qquad \frac{1}{\tau_{mn}} = \frac{V_{mn}^2}{|v|}$$

$$\Delta_{eff,m} \approx \Delta_m + \sum_{n \neq m} \left(\frac{1}{\tau}\right)_{mn} e^{i\,\arg(\Delta_n)}$$

- To be affected by a channel, need to be able to scatter into it
- Once scattered into it, the phase of its pairing potential matters.

Particular cases:

- Disorder scattering into the pairing partner – necessarily reduces Δ_{eff} (phase difference of π).

$$\Delta_m c_m^+ c_{-m}^+ \quad \Rightarrow \quad \Delta_m = -\Delta_{-m}$$

- Delocalizes Majorana modes in p-wave superconductors.

- Different situation for s-wave superconductors
  - Selection rule – disorder does not flip spin, so no scattering to pairing partner.
  - No phase difference of pairing potentials.

  - Disorder enhances localization

In our case, large k behaves like s-wave, small k behaves like p-wave

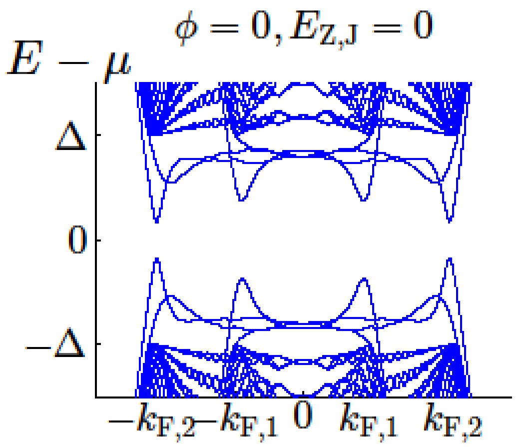

The small k determines topology, the large k determines localization.

Magnetic impurities couple large-k pairing partners, and delocalize the Majorana modes

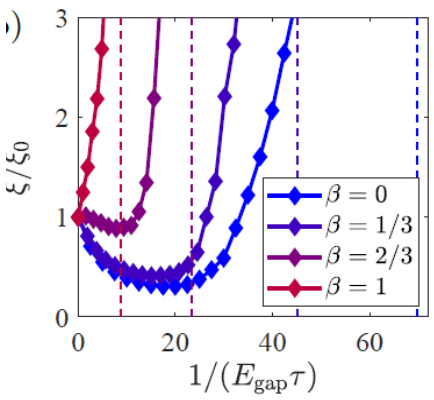

Manipulating and braiding the Majorana zero modes

With Erez Berg (Chicago, WIS)

Perpendicular magnetic field makes the phase vary along the junction

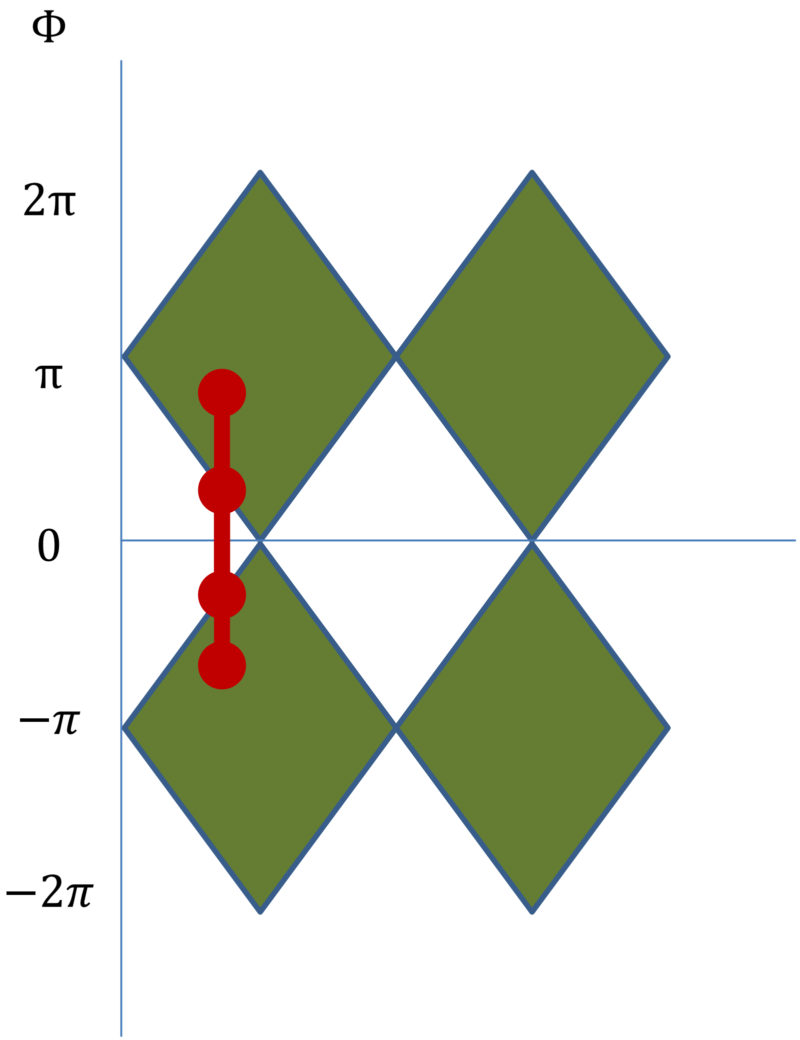

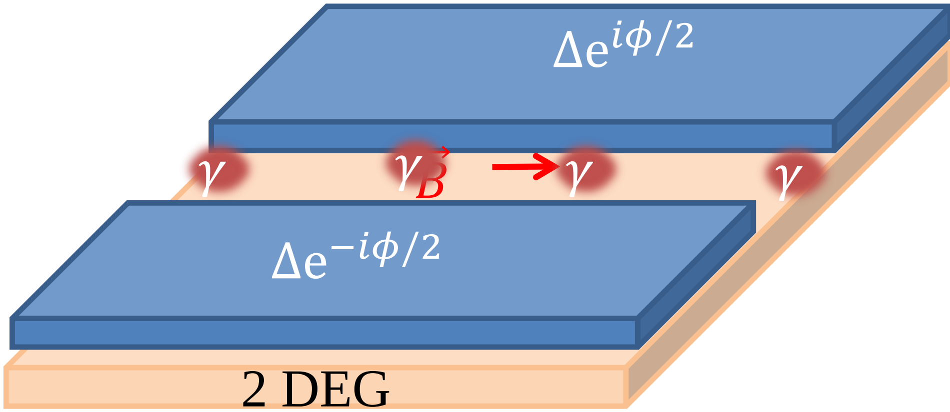

Four Majorana zero modes –

two at the junction ends, two movable by $B_\perp$

The two zero modes at the interior may be moved by varying the magnetic field, or by driving a supercurrent through the junction.

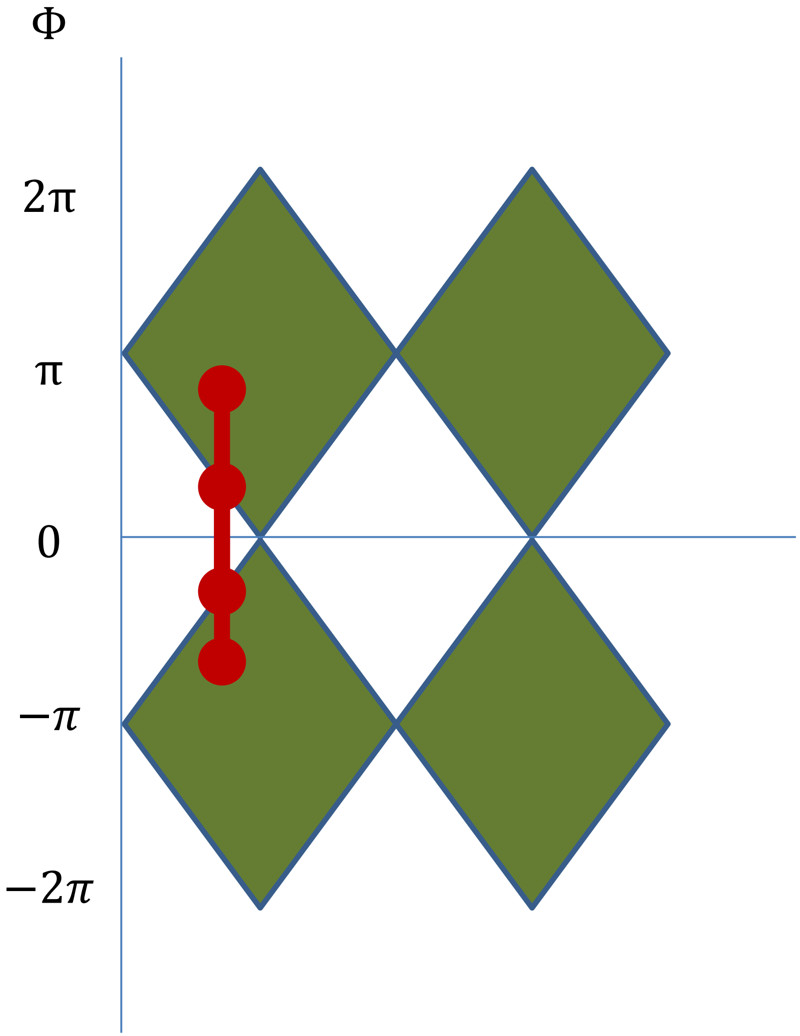

$B_{\perp}$ stretches the covered range of ϕ, while supercurrent shifts it.

Detour - Screening currents and Josephson vortices

- A super-conductor accommodates a magnetic field in the form of circular vortices formed due to magnetic field generated by circulating super-currents. A vortex involves 2π phase winding and one flux quatum $\frac{hc}{2e}$.

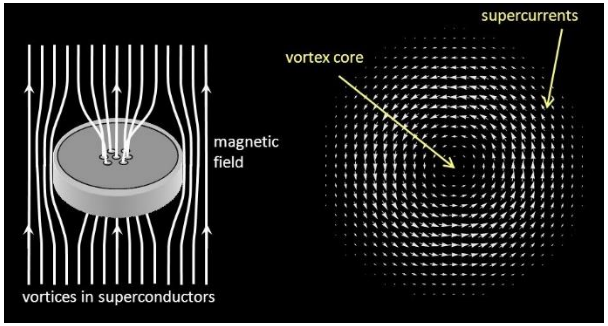

- A Josephson junction is a very anisotropic super-conductor, so the vortices are elongated

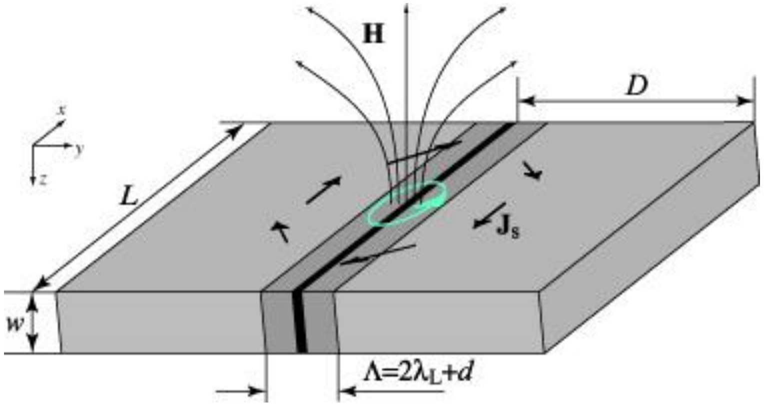

Screening current and phase configuration

- In a Josephson junction, the phase configuration is determined by balancing the magnetic energy, $(\partial_x \phi)^2$, with the Josephson energy $V(\phi)$.
- For an SIS junction,

$$V(\phi) = (1 - \cos\phi),$$

the phase satisfies a Sine-Gordon equation, and the vortex is a Sine-Gordon soliton.

- Generally, the soliton is the trajectory between two minima of $V(\phi)$. Follows $\partial_x^2 \phi = V'(\phi)$
- Here, $V(\phi)$ is more complicated, and is determined by the parallel magnetic field.

Roughly, we need to minimize

$$-\left|\cos(\phi_B + {}^{\phi}/_{2})\right| - \left|\cos(\phi_B - {}^{\phi}/_{2})\right|$$

First order phase transition at $\phi_B = \pi/4$ – the system tunes itself into a topological phase.

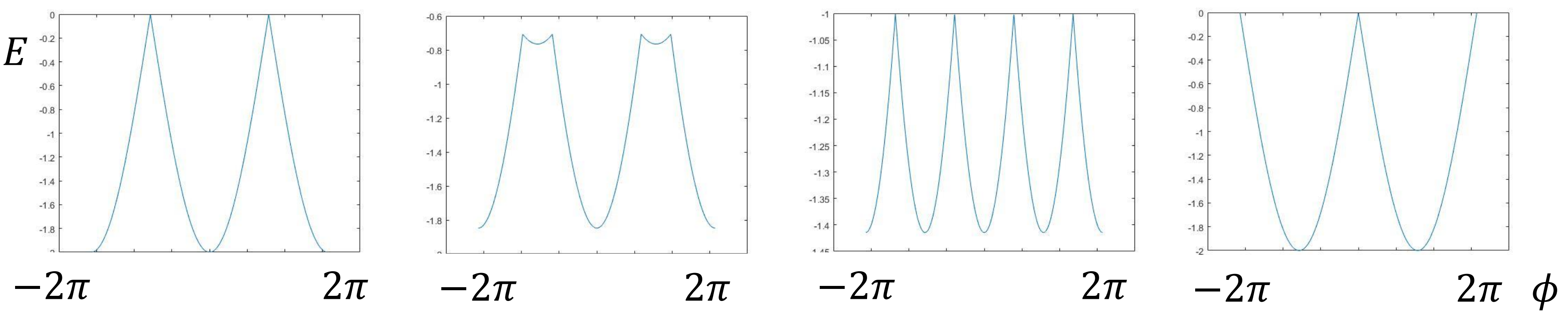

$\phi_B = 0$ $\qquad$ $\phi_B = \frac{\pi}{8}$ $\qquad$ $\phi_B = \frac{\pi}{4}$ $\qquad$ $\phi_B = \frac{\pi}{2}$

At the transition point, $V(\phi)$ has a period of π rather than 2π, so the soliton is halved – a π vortex.

The π-vortex separates between trivial and topological regions – carries a zero mode. A 2π vortex carries two zero modes.

What do we have so far?

- Trivial/topological phases tuned by phase difference/parallel field. Topological phase has end modes.
- Extra Majorana zero modes created by perpendicular magnetic field.
- Majorana zero modes movable by perpendicular field/supercurrent

Calls for a scheme for braiding!

The current-driven tri-junction braiding scheme:

Braiding in $1 + \epsilon$ dimensions
Alicea et al., many follow-ups

For the planar Josephson junction –
Hell, Flensberg, Leijnse

The knobs:

- Parallel magnetic field
- Perpendicular magnetic field
  (assume $L \ll \lambda_J$, no screening currents)

fixed

- Currents – time dependent

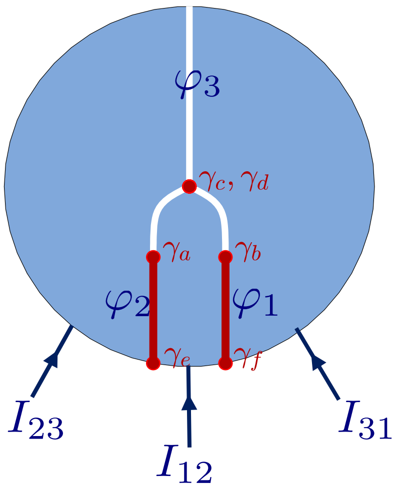

The single junction:

- In the absence of screening currents the phase varies linearly with position, with the slope determined by the perpendicular magnetic field.
- Limit ourselves to 0-2 MZMs per arm

phase

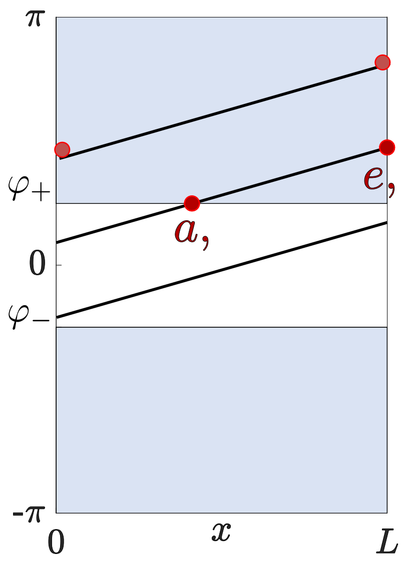

position

The tri-junction –

1. Quantization of the vorticity at the center

$$\varphi_1(x_1=0)+\varphi_2(x_2=0)+\varphi_3(x_3=0)=2\pi n$$

2. Continuity of the magnetic field at the center

$$\partial_x\varphi_1(x_1=0)=\partial_x\varphi_2(x_2=0)=\partial_x\varphi_3(x_3=0)$$

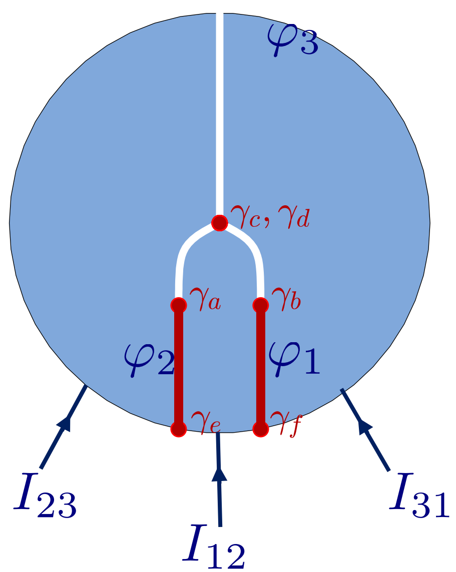

The plane of no-vortex at the center

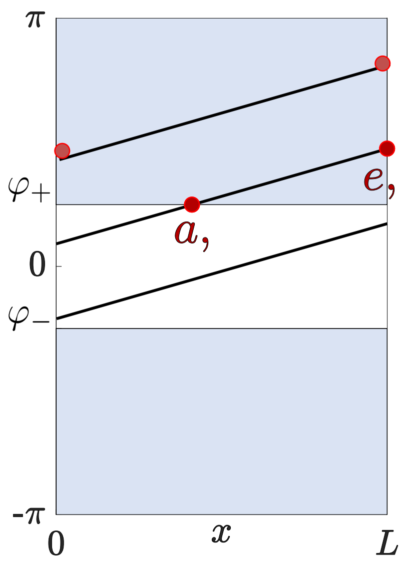

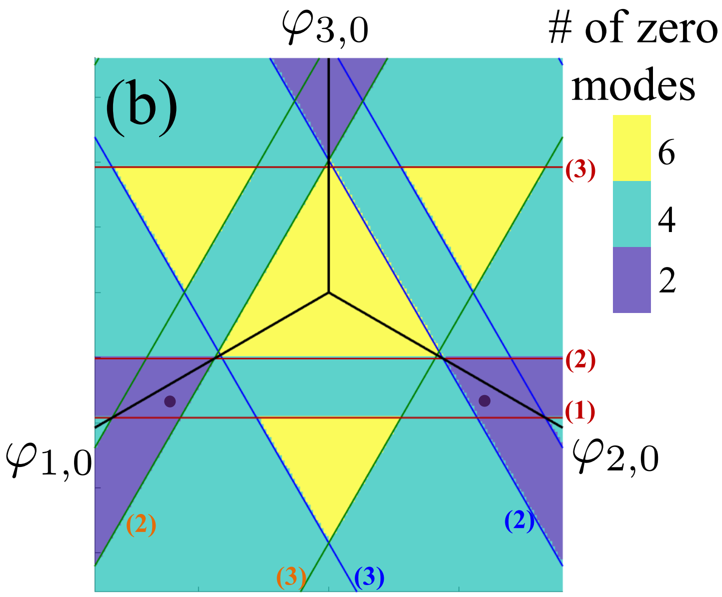

A topological manipulation – motion along a trajectory that cannot be contracted to a point

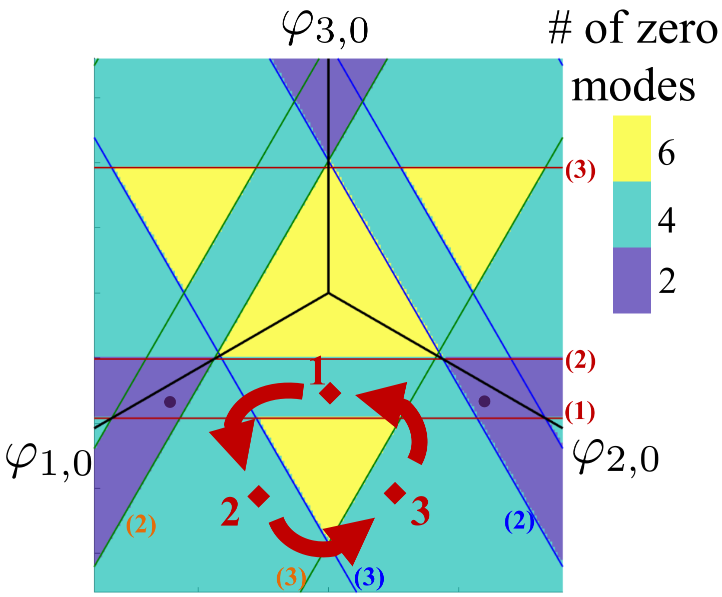

Current minimizes $I_i\varphi_i + V(\varphi_i)$

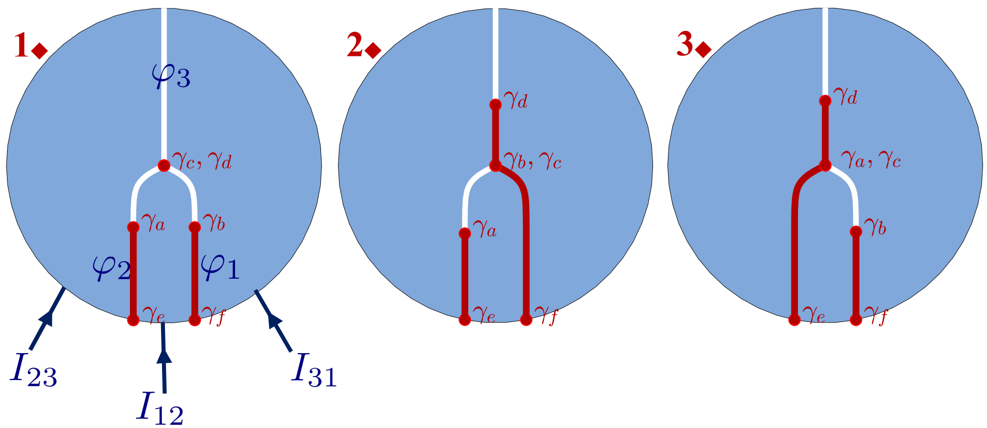

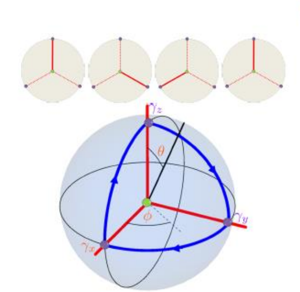

Sau et al,
Karzig et al. 2016

Can be looked at as six zero modes, out of which two are coupled

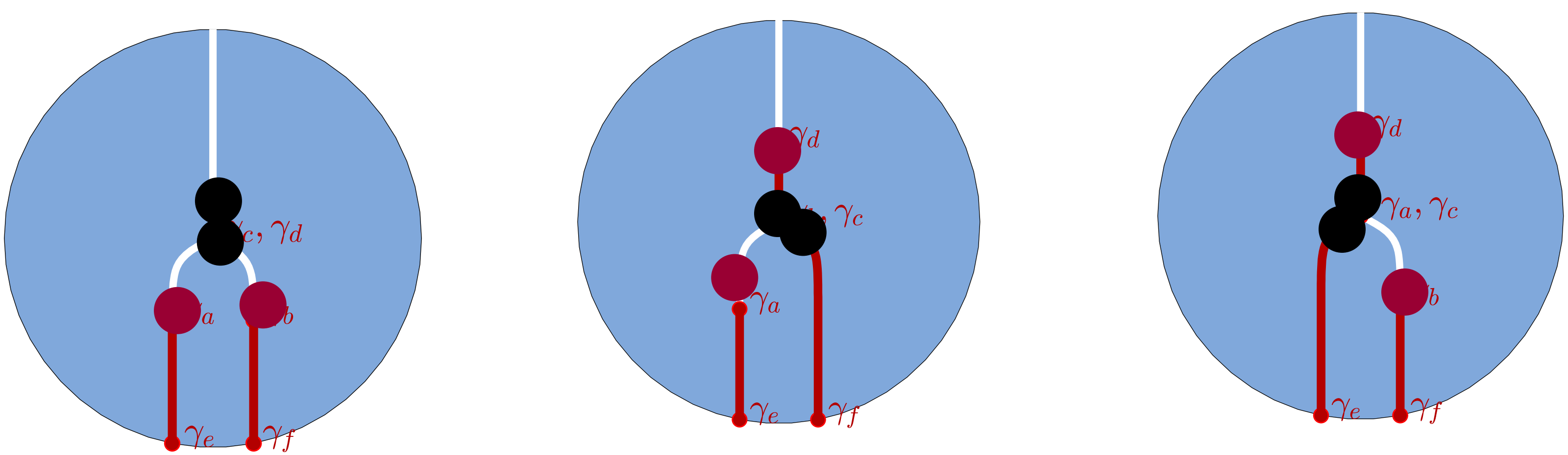

Summary

1. The relative phase is a user-friendly parameter to use on the way to topological superconductivity.
2. First-order phase transition where the system self tunes itself to the topological regime.
3. Fractionalization of the Josephson vortex at the phase transition.
4. Disorder localizes the Majorana modes.
5. Scheme for Majorana braiding.

The current-driven tri-junction braiding scheme:

Braiding in $1+\epsilon$ dimensions
Alicea et al., many follow-ups

For the planar Josephson junction –
Hell, Flensberg, Leijnse

The knobs:

- Parallel magnetic field
- Perpendicular magnetic field
  (assume $L \ll \lambda_J$, no screening currents)

fixed

- Currents – time dependent

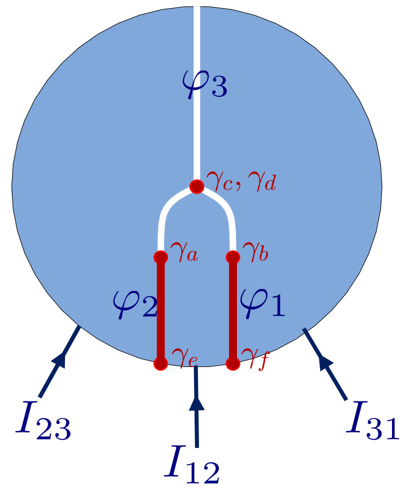

The single junction:

- In the absence of screening currents the phase varies linearly with position, with the slope determined by the perpendicular magnetic field.
- Limit ourselves to 0-2 MZMs per arm

phase

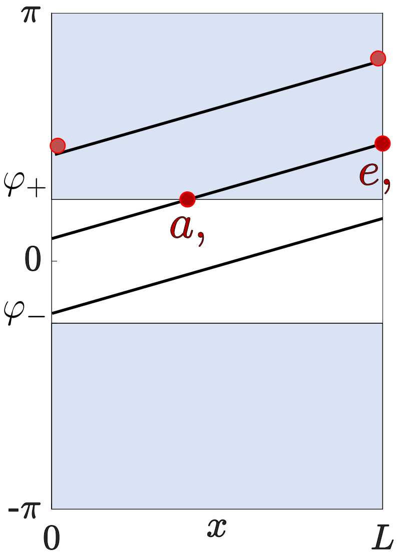

position

The tri-junction –

1. Quantization of the vorticity at the center

$$\varphi_1(x_1 = 0) + \varphi_2(x_2 = 0) + \varphi_3(x_3 = 0) = 2\pi n$$

2. Continuity of the magnetic field at the center

$$\partial_x \varphi_1(x_1 = 0) = \partial_x \varphi_2(x_2 = 0) = \partial_x \varphi_3(x_3 = 0)$$

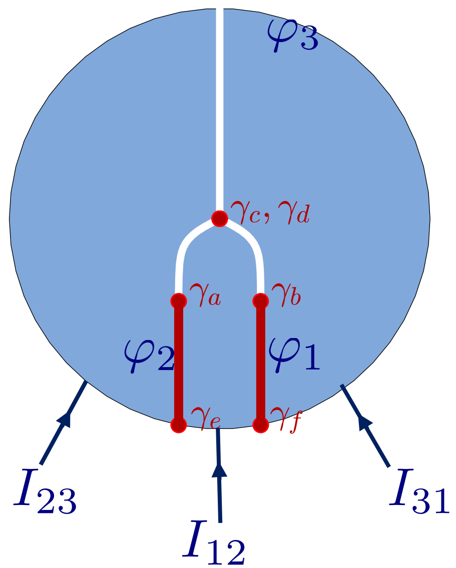

The plane of no-vortex at the center

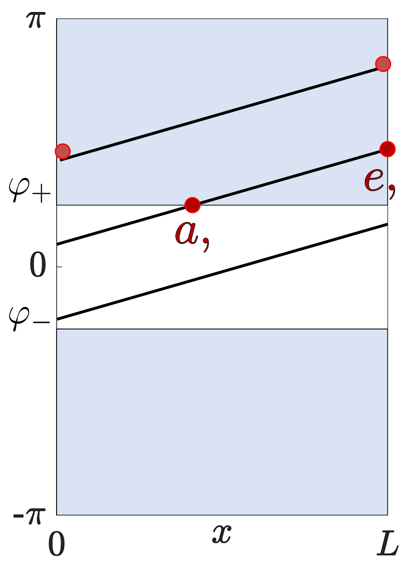

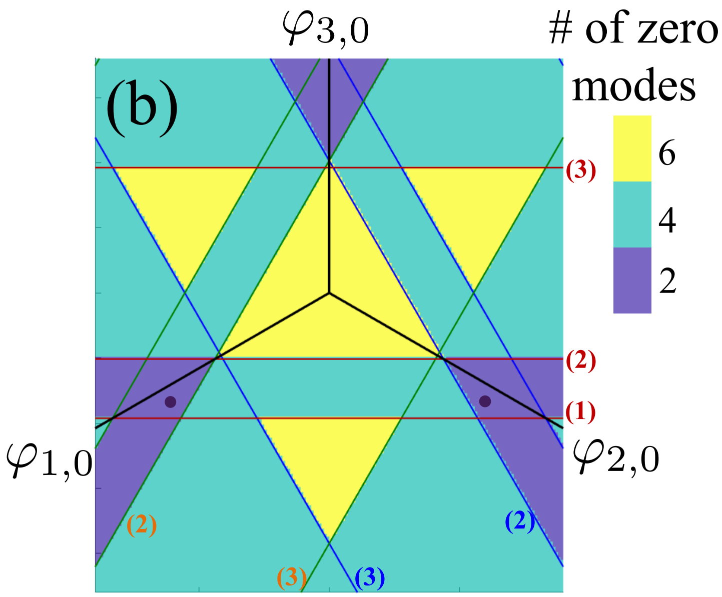

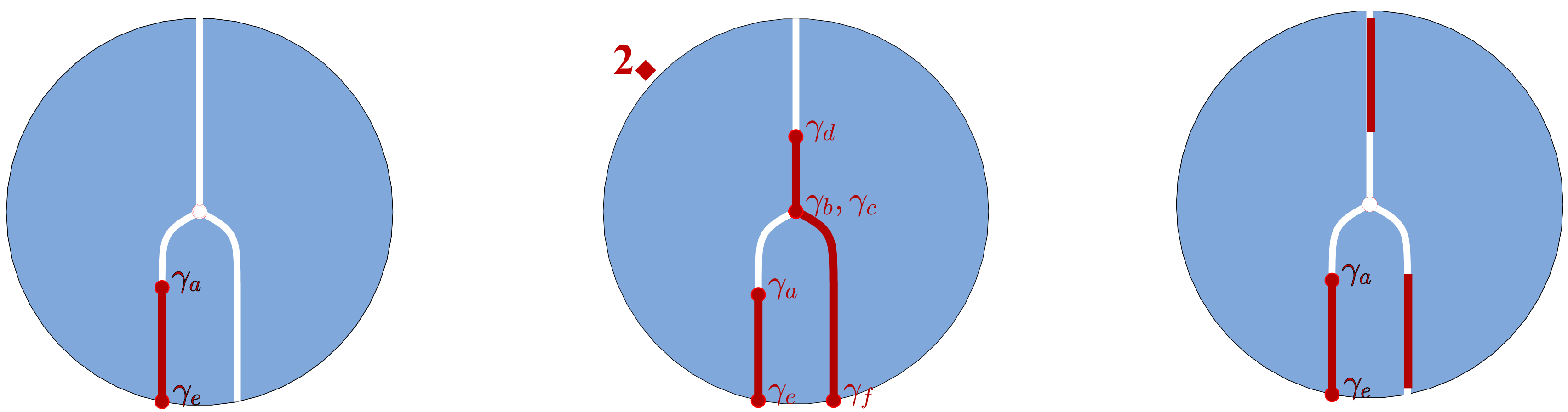

A topological manipulation – motion along a trajectory that cannot be contracted to a point

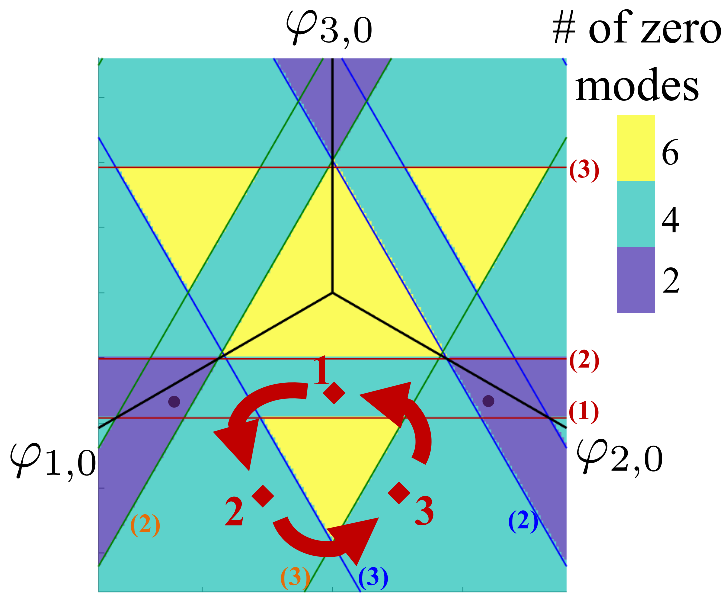

Current minimizes $I_i\varphi_i + V(\varphi_i)$

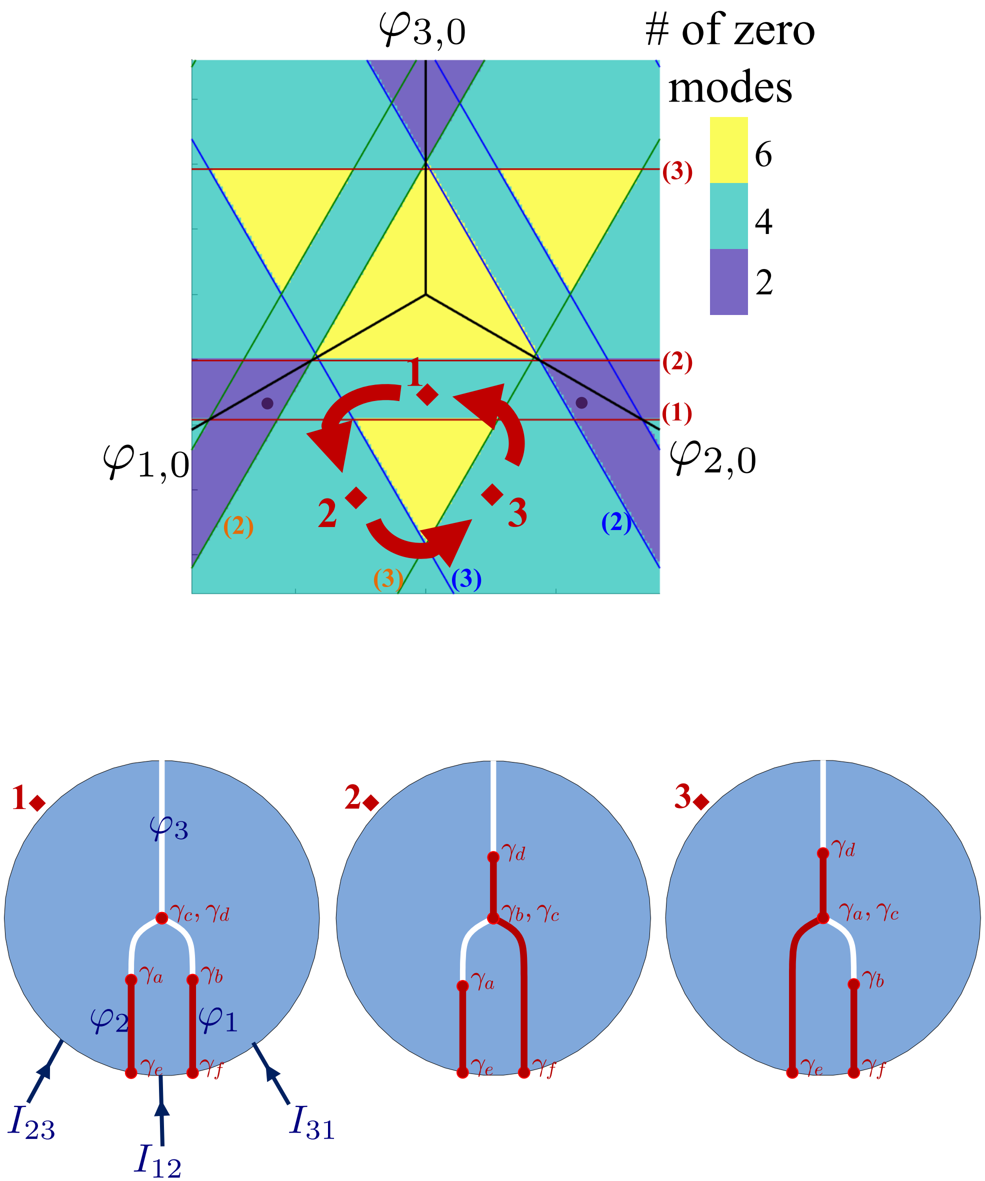

$\varphi_{3,0}$
# of zero modes
6
4
2
(3)
(2)
(1)
$\varphi_{1,0}$
$\varphi_{2,0}$
1
2
3
(2)
(3)
(3)
(2)
1
φ_3
γ_c, γ_d
γ_a
γ_b
φ_2
φ_1
γ_e
γ_f
I_{23}
I_{12}
I_{31}
2
γ_d
γ_b, γ_c
γ_a
γ_e
γ_f
3
γ_d
γ_a, γ_c
γ_b
γ_e
γ_f

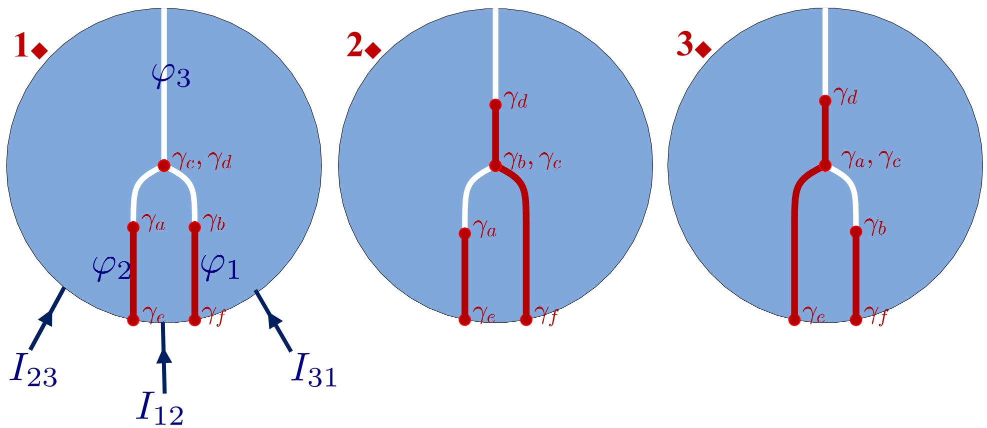

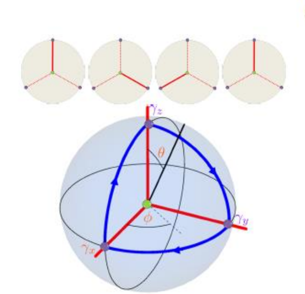

Karzig et al. 2016

Can be looked at as six zero modes, out of which two are coupled